ICARUS 20, 146–152 (1973)

On the Interpretation of the "Inverse Phase Effect" for CO_2 Equivalent Widths on Venus

LAIRD P. WHITEHILL AND JAMES E. HANSEN

Goddard Institute for Space Studies, New York, New York 10025

Received May 2, 1973

Computations of the equivalent widths of absorption lines as a function of planetary phase angle are made for a homogeneous cloud with particles having the properties (shape, refractive index, and size distribution) deduced from polarimetry of Venus. The computed equivalent widths show an 'inverse phase effect' comparable to that which is observed for CO_2 lines on Venus. This result verifies a recent suggestion of Regas *et al.* that the existence of an inverse phase effect does not by itself imply the presence of multiple layers of scattering particles in the atmosphere of Venus.

INTRODUCTION

Observations of the equivalent widths of CO_2 lines on Venus suggest a decrease in the equivalent width toward small phase angles (superior conjunction). The most complete published observations are those of Young *et al.* (1971; cf. their Fig. 12) and Young (1972, their Figs. 4–9). The equivalent widths of the 7820Å CO_2 bands appear to be 10–30% less for phase angles in the range 0–30° than for phase angles of 50–80°. Although the phase variation is uncertain, due to comparable day-to-day fluctuations in the measured equivalent widths, it has nevertheless been used as the basis for definitive claims about the structure of the clouds of Venus.

Venus is observed to be veiled by clouds or haze, so the absorption lines in reflected solar light must be formed in or above a scattering atmosphere. It has been shown that, for a homogeneous atmosphere with isotropic scattering, the equivalent widths of absorption lines will decrease monotonically with increasing phase angle (Chamberlain and Kuiper, 1956; Chamberlain and Smith, 1970). Thus the inverse phase effect, if it is real, implies either that the scattering is anisotropic or that the atmosphere is inhomogeneous (or both).

Of course, in reality, both complications exist on Venus: The scattering is anisotropic and the atmosphere is inhomogeneous. But *if* it could be shown that anisotropic scattering does not cause an inverse phase effect, then the observed phase effect could more easily be used to investigate the vertical structure of the atmosphere. This supposedly has been done. Hunt (1972a, b) has made extensive computations for spherical cloud and haze particles. For the case of a homogeneous atmosphere, he finds that "... the phase curves computed with this model are always smooth, monotone decreasing functions of the phase angle ..." (Hunt, 1972a).

Regas *et al.* (1973) have called this result to question. Hunt's conclusion is not consistent with the computations of Hansen (1969) which showed a decreased line depth at small phase angles for a scattering diagram[1] with a backward lobe. Regas *et al.* integrated line profiles computed by Hansen to obtain the equivalent widths at several phase angles; they showed that an inverse phase effect exists for the particular scattering diagram employed, which was appropriate for terrestrial water

[1] In this paper we use the terminology 'scattering diagram' instead of the more common 'phase function' in order to avoid confusion with 'phase effect'.

clouds. Unpublished computations of Regas, made with an approximate computational method including the effects of inhomogeneity, show a similar effect.

Calculations

It is possible to make computations with scattering diagrams which are much more relevant to the atmosphere of Venus. It has been shown from the linear polarization of sunlight reflected from Venus that the "cloud" particles are spherical with a refractive index ~1.43 (for wavelengths 0.8–1 μm) and a mean particle radius ~1 μm (Hansen and Arking, 1971; Hansen and Hovenier, 1973).

The scattering diagram we employ here was computed for $\lambda = 7820$ Å, $n_r = 1.43$, $n_i = 0$, and the particle size distribution (Hansen, 1971b).

$$n(r) = \text{constant}\, r^{(1-3b)/b} e^{-r/ab}. \qquad (1)$$

a, the mean effective radius, was 1.05 μm, and b, the effective variance, was 0.07. The integration over particle size was for the range (0–4 μm), which, for the distribution employed, is practically equivalent to the range (0–∞). The integration was made with a sufficient number of points (~10^3) to assure convergence. The resulting scattering diagram is shown by the solid curve in Fig. 1. Results are also shown for $n_r = 1.41$ and 1.45 in order to illustrate the magnitude of the uncertainty in the scattering diagram of the Venus cloud particles; the value 0.02 is the maximum uncertainty in n_r, not a probable error. Variations in the scattering diagram due to uncertainties in the size distribution are comparable to those illustrated in Fig. 1.

Thus it is clear that the scattering diagram for the Venus clouds has backward lobes for scattering angles 150–180°, at least for the region of the atmosphere responsible for the polarization and absorption lines of reflected sunlight. The peak at scattering angles ~160° is the 'rainbow' which is due to light internally reflected once inside the cloud particles, while the peak at 180° is the "glory" which arises from the edge rays striking the cloud particles (cf. van de Hulst, 1957; Hansen. 1972).

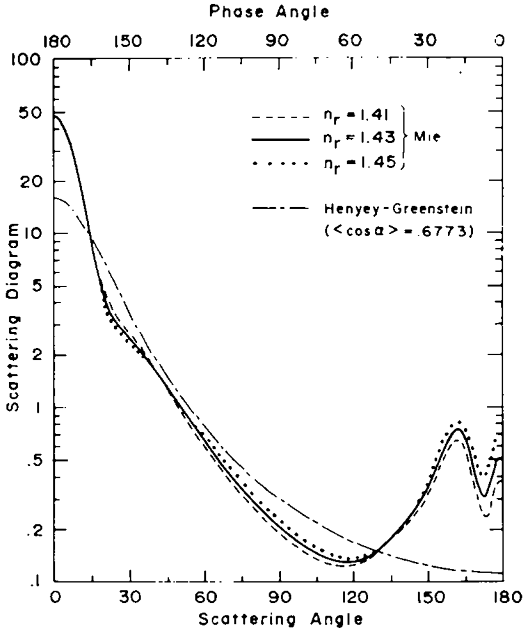

Fig. 1. Scattering diagrams used for multiple scattering computations. The Mie results are for the indicated values of refractive index, with all three for $\lambda = 7800$ Å and the size distribution (1). The Henyey-Greenstein scattering diagram is for an asymmetry parameter, $\langle \cos \alpha \rangle$, the same as that of the Mie scattering diagram for $n_r = 1.43$.

Let σ = scattering coefficient per unit volume, k_c = absorption coefficient per unit volume in the continuum (which may be due to absorption in the scattering particles), and k_ν = additional absorption coefficient per unit volume (due to the gas causing the absorption line). The single-scattering albedo at the frequency ν is then

$$\tilde{\omega}_\nu = \sigma/(k_\nu + k_c + \sigma). \qquad (2)$$

The single-scattering albedo in the continuum is

$$\tilde{\omega}_c = \sigma/(k_c + \sigma), \qquad (3)$$

which is assumed to be constant over an absorption line. For the Lorentz line shape

$$k_\nu = k_0\left[1 + \left(\frac{\nu - \nu_0}{\gamma}\right)^2\right]^{-1}, \qquad (4)$$

where γ is the Lorentz width of the line. If the single-scattering albedo at the line center in the absence of continuous absorption is represented by $\tilde{\omega}_0$,

$$\tilde{\omega}_0 = \sigma/(k_0 + \sigma), \tag{5}$$

then $\tilde{\omega}_\nu$ may be expressed as

$$\tilde{\omega}_\nu = \left[\frac{1}{\tilde{\omega}_c} + \frac{1 - \tilde{\omega}_0}{\tilde{\omega}_0(1 + x^2)}\right]^{-1} \tag{6}$$

where $x \equiv (\nu - \nu_0)/\gamma$.

The equivalent width of an absorption line is

$$W = \int_0^\infty \frac{I_c - I_\nu}{I_c} \mathrm{d}\nu, \tag{7}$$

where I_c and I_ν are the intensity in the continuum and at the frequency ν within the line. Thus for a Lorentz line

$$W(\tilde{\omega}_c, \tilde{\omega}_0) \simeq 2\gamma \int_0^\infty \frac{I_c(\tilde{\omega}_c) - I_\nu(\tilde{\omega}_c, \tilde{\omega}_0, x)}{I_c(\tilde{\omega}_c)} \mathrm{d}x \tag{8}$$

We computed reflected intensities for a homogeneous atmosphere using the doubling method, which has been described many times in the literature (e.g., Hansen, 1971a; Whitehill, 1972). The results were integrated over the illuminated part of the planetary disk[2] using the method of Horak (1950). The computations were made with a continuum single-scattering albedo, $\tilde{\omega}_c$, which would yield a spherical (Bond) albedo of ~92% in the continuum, the same spherical albedo as that assumed by Hunt (1972b; cf. his Table 2 and Fig .2); a series of photoelectric observations summarized by Irvine (1968) indicates that this is approximately the spherical albedo of Venus for $\lambda \sim 8000$ Å. For the Mie scattering diagram with $n_r = 1.43$ this required $\tilde{\omega}_c \sim 0.99956$; the anisotropy parameter[3] for this scattering diagram is $\langle\cos\alpha\rangle \sim 0.6773$. Computations were also made with the Heney-Greenstein scattering diagram,

$$p(\alpha) = \frac{1 - \langle\cos\alpha\rangle^2}{(1 + \langle\cos\alpha\rangle^2 - 2\langle\cos\alpha\rangle\cos\alpha)^{3/2}} \tag{9}$$

using the same values of $\tilde{\omega}_\nu$ and $\langle\cos\alpha\rangle$ as for the Mie scattering diagram. Finally, computations were made for isotropic scattering with the $\tilde{\omega}_\nu$ defined above modified according to the similarity relation

$$\tilde{\omega}_\nu^{\text{iso}} = 1 - \frac{1 - \tilde{\omega}_\nu}{1 - \langle\cos\alpha\rangle} \tag{10}$$

with $\langle\cos\alpha\rangle = 0.6773$.

Figure 2 shows the relative equivalent widths computed for the three scattering diagrams. These are each normalized to unity at the phase angle where the maximum value occurs. Figure 2 was obtained from computations for $\tilde{\omega}_0 = 1/(1 + 0.1)$, but for $\tilde{\omega}_0 = 1/(1 + 1)$ and $\tilde{\omega}_0 = 1/(1 + 10)$ the results are practically the same as those illustrated; thus within this range the conclusions are not sensitive to line strength.

The major contribution to the equivalent width comes from the wings of the lines. However, with actual observations it is usually impossible to measure the entire equivalent width because of the overlapping of lines and the consequent difficulty in defining the true continuum. Thus in Fig. 3 we have also illustrated the results of computations (for the Mie scattering diagram, $n_r = 1.43$) in which the integration for the equivalent width was from I_ν to $0.99 I_c$ and from I_ν to $0.75 I_c$. For the latter case, the shaded part of the insert in Fig. 3 indicates the area included in the equivalent width. The uniformly depressed continuum which we have considered in Fig. 3 does not provide an accurate representation of some practical

[2] Integrations were also made along a line on the planetary disk to simulate a given spectrometer slit orientation on the planet, as discussed in the last paragraph of this section.

[3] $\langle\cos\alpha\rangle$ is the average value of $\cos\alpha$ weighted by the scattering diagram, $p(\alpha)$,

$$\langle\cos\alpha\rangle = \tfrac{1}{2}\int_{-1}^{1} p(\alpha)\cos\alpha \,\mathrm{d}(\cos\alpha),$$

where α is the scattering angle. For isotropic scattering the single scattering albedo ($\tilde{\omega}_c^{\text{iso}}$) corresponding to an assumed spherical albedo can be found in Table A1 of Chamberlain and Smith (1970). The value of $\tilde{\omega}_c$ which will yield approximately the same spherical albedo for anisotropic scattering then follows from $\langle\cos\alpha\rangle$ and the similarity relation (Hansen, 1969):

$$\tilde{\omega}_c = 1 - (1 - \langle\cos\alpha\rangle)(1 - \tilde{\omega}_c^{\text{iso}})$$

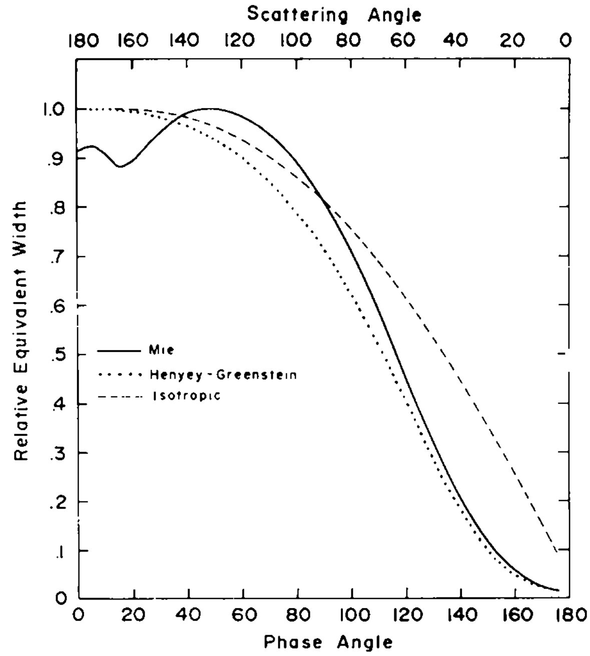

FIG. 2. Equivalent widths for a Lorentz absorption line. The Henyey-Greenstein and Mie ($n_r = 1.43$) scattering diagram used in the computations are shown in Fig. 1. The calculations were for $\tilde{\omega}_0 = 1/(1 + 0.1)$, corresponding to a line of intermediate strength. The results for each scattering diagram are normalized to unity at the phase angle of maximum equivalent width.

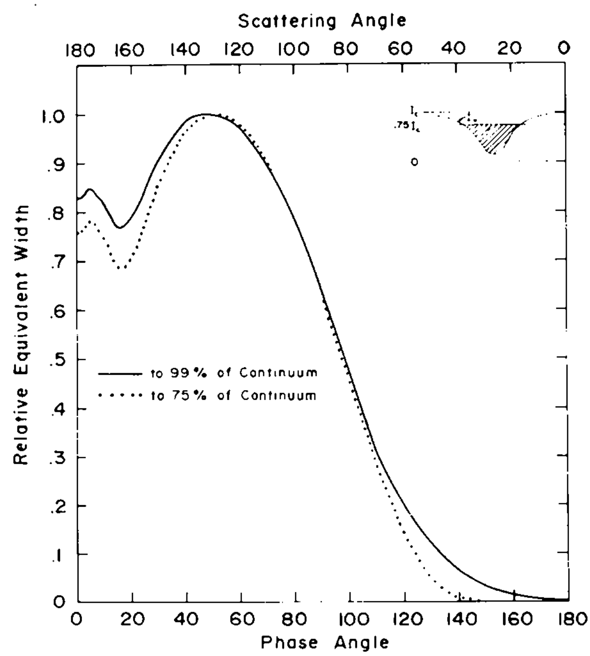

FIG. 3. Equivalent width of a Lorentz absorption line, as in Fig. 2. The results are for the Mie scattering diagram ($n_r = 1.43$), but the area included in the equivalent width is limited to that below $0.99I_c$ and $0.75I_c$. The insert on the upper right is a schematic indication of the area included for the integration to $0.75I_c$.

problems which arise in measurements of equivalent widths (A. Young, private communication), but a comparison of Figs. 3 and 2 is nevertheless sufficient to (1) illustrate that an inverse phase effect can be expected even if the continuum is not precisely known, and (2) illustrate that an accurate measurement of the phase effect would require a very accurate knowledge of the true continuum.

From Figs. 2 and 3 it is obvious that the equivalent width as a function of phase angle depends markedly on the shape of the scattering diagram. An "inverse phase effect" exists for the Mie scattering diagram, and it is clear that this is a direct result of the shape of the scattering diagram: indeed, if Fig. 1 is turned upside-down and compared to the other figures, the close correspondence is even clearer (but note that the vertical scale is logarithmic in Fig. 1). The inverse phase effect is clearly due to the backward peaks (the rainbow and glory) in the scattering diagram; at their scattering angle these features cause an increase in the percentage of single scattered photons and a corresponding decrease in the percentage of photons with a long total pathlength in the atmosphere.

The results which we have illustrated are for the intensity integrated over the visible part of the planet. We have also examined the distribution of intensity over the planetary disk, and we have made integrations along a line on the disk to represent a given spectrometer slit orientation. In the latter case the inverse phase effect may be somewhat stronger or weaker than in the case of the integration over the visible disk, with the results depending on the slit location. For the most convenient slit location, along the intensity equator, the relative equivalent width is nearly the same (within ~0.03) as for the disk-integrated results in Figs. 2 and 3 (for the same values of $\tilde{\omega}_0$ and other parameters).

Discussion

The results which we have presented illustrate that a signature or imprint of the scattering diagram is carried by the phase variation of the equivalent width of absorption lines. The correspondence is so straightforward that it would seem natural to try to invert measured equivalent widths for Venus (which can be observed at all phase angles) to extract the scattering diagram. However, in practice, this will be difficult because of the day-to-day variations which exist in the equivalent widths and because of the comparable magnitude of effects due to atmospheric inhomogeneities. These difficulties are illustrated by a comparison of Fig. 12 of Young *et al.* (1971), Figs. 2 and 3 of our paper, and Fig. 9 of Hunt (1972b). It is very unlikely that the scattering diagram can be deduced from equivalent widths with an accuracy comparable to that which can be obtained indirectly through the polarization.

But since the scattering diagram is already accurately known from the polarization, it would seem more promising to try to use the variation of equivalent width with phase angle as a tool for investigating the vertical atmospheric structure. We want to emphasize that such studies must incorporate an accurate representation of the scattering diagram. Regas *et al.* (1973) have made a similar statement. However, even if a reliable scattering diagram is employed, such studies will still be hampered by the difficulty in measuring equivalent widths and their day-to-day variations. A greater potential for investigating atmospheric structure may be provided by *line profiles*; because, in principle, the profile of an entire band can be measured at one time, the results are not as sensitive to the shape of the scattering diagram as they are for equivalent widths, and the effects of temperature and pressure vary from line to line within a band in a predictable fashion. Preliminary reports of studies of line profiles of Venus (Traub, 1971; Carleton *et al.*, 1971) support the assumption that the line profiles can yield information on atmospheric structure, but adequate details of this work have not been published yet.

For problems in absorption line formation, the atmosphere of Venus is certainly inhomogeneous in the vertical direction due to variations of temperature and pressure. It is probable that there are also significant changes in the scattering properties with height: maps of thermal emission demonstrate that there is a continuous cloud cover with substantial optical density at a temperature level ~230K (corresponding to a pressure ~200mb); and transits of Venus across the sun and the extension of the 'horns' of Venus at small phase angles indicate that there are more diffuse (i.e., haze) particles higher in the atmosphere, at pressures as low as ~5mb (cf. the reviews by Hunten, 1971 and Rea, 1972). Thus in detailed theoretical studies the effects of inhomogeneities must be investigated. Our computations reported here were made with a homogeneous atmosphere only so that the phase effect due to the shape of the scattering diagram could be isolated. Even if the "inverse phase effect" for absorption lines on Venus (assuming that there is one) is primarily due to the shape of the scattering diagram, we should still not expect our computations to agree with observations for large phase angles; any gas above the clouds would tend to keep the equivalent width from decreasing at large phase angles as rapidly as it does in the computations illustrated here.

Acknowledgments

We thank Dr. J. Regas and his coauthors for a preprint of their paper, Dr. L. Young and Dr. A. Young for comments on our paper and discussions of their observations, and Dr. G. Hunt for explanations concerning his computations.

References

Carleton, N. P., Traub, W. A., and Wattson, R. B. (1971). Venus CO_2 line profiles: Observations compared with predictions for a variety of cloud distributions. *Bull. Amer. Astron. Soc.* **3**, 278.

Chamberlain, J. W., and Smith, G. R. (1970). Interpretation of the Venus CO_2 absorption bands. *Astrophys. J.* **160**, 755–765.

Chamberlain, J. W., and Kuiper, G. P. (1956). Rotational temperature and phase variation of the carbon dioxide bands of Venus. *Astrophys. J.* **139**, 399–405.

Hansen, J. E. (1969). Absorption-line formation in a scattering planetary atmosphere: A test of van de Hulst's similarity relations. *Astrophys. J.* **158**, 337-349.

Hansen, J. E. (1971a). Multiple scattering of polarized light in planetary atmospheres. Part I. The doubling method. *J. Atmos. Sci.* **28**, 120-125.

Hansen, J. E. (1971b). Multiple scattering of polarized light in planetary atmospheres. Part II. Sunlight reflected by terrestrial water clouds. *J. Atmos. Sci.* **28**, 1400 1426.

Hansen, J. E. (1972). Information contained in the intensity and polarization of scattered sunlight. Report, NASA Institute for Space Studies, New York.

Hansen, J. E., and Arking, A. (1971). Clouds of Venus: Evidence for their nature. *Science* **171**, 669 672.

Hansen, J. E., and Hovenier, J. W. (1973). Interpretation of the polarization of Venus. *J. Atmos. Sci.* (to be submitted).

Horak, H. G. (1950). Diffuse reflection by planetary atmospheres. *Astrophys. J.* **112**, 445-463.

Hunt, G. E. (1972a). Formation of spectral lines in planetary atmospheres. 1. Theory for cloudy atmospheres; application to Venus. *J. Quant. Spectrosc. Radiat. Transfer* **12**, 387–404.

Hunt, G. E. (1972b). Formation of spectral lines in a planetary atmosphere. II. Spectroscopic evidence for the structure of the visible Venus clouds. *J. Quant. Spectrosc. Radiat. Transfer* **12**. 405-419.

Hunten, D. M. (1971). Composition and structure of planetary atmospheres. *Space Sci. Rev.* **12**, 539–599.

Irvine, W. M. (1968). Monochromatic phase curves and albedos for Venus. *J. Atmos. Sci.* **25**, 610–616.

Rea, D. G. (1972). Composition of the upper clouds of Venus. *Rev. Geophys. Space Phys.* **10**, 369-378.

Regas, J. L., Boese, R. W., Giver, L. P., and Miller, J. H. (1973). Does spectroscopic evidence require two scattering layers in the Venus atmosphere? *J. Quant. Spectrosc. Radiat. Transfer* **13**, 461–463.

Traub, W. (1971). Line profiles. Paper presented at the Conference on Upper Atmosphere of Venus, Calif. Inst. of Technol., Pasadena, CA, May 5–6.

van de Hulst, H. C. (1957). "Light scattering by small particles." Wiley, New York.

Whitehill, L. P. (1972). Solar system applications of Mie theory and of radiative transfer of polarized light. Ph.D. Thesis, Cornell University.

YOUNG, L. D. G. (1972). High resolution spectra of Venus—a review. *Icarus* **17**, 632.

YOUNG, L. D. G., SCHORN, R. A. J., BARKER, E. S., AND WOSZCZYK, A. (1971). High dispersion spectroscopic observations of Venus during 1968 and 1969. I. The carbon dioxide bands at 7820 Å. *Acta Astron.* **21**, 329–363.